

# Analysis of cascaded H-bridge multilevel inverter with current control methods

Prem Sunder Gnanamurthy<sup>1</sup>, Veerapathiran Govindasamy<sup>2</sup>

<sup>1</sup>Department of Electrical and Electronics Engineering College, Mailam Engineering College, India

<sup>2</sup>Department of Innovation and Technology, Learning Links Foundation, India

## Article Info

### Article history:

Received Aug 30, 2021

Revised Mar 2, 2022

Accepted Mar 25, 2022

### Keywords:

Hysteresis controller

MATLAB Simulink

Multilevel inverter

PI controller

Predictive controller

## ABSTRACT

A detailed model and analysis of a five-level cascaded H-bridge (CHB) multilevel inverter with different current control methods are presented. Simulation models of the CHB inverter with hysteresis current controller, PI current controller using SPWM technique and predictive current controller have been built to demonstrate the CHB inverter system performance with regard to load current THD and reference current tracking. In controlling the load current, the hysteresis and the PI current controllers have the problem of current ripple and phase lag, respectively. The proposed predictive current control method effectively addresses these issues. The current control methods are analyzed for varying reference current and unbalanced load conditions. The simulation results are observed and analyzed using the MATLAB Simulink software to validate the current control methods.

*This is an open access article under the [CC BY-SA](#) license.*



## Corresponding Author:

Prem Sunder Gnanamurthy

Department of Electrical and Electronics Engineering, Mailam Engineering College

Mailam, Tamil Nadu 604304, India

Email: premgsunder@gmail.com

## 1. INTRODUCTION

In modern days, plentiful industries have initiated to utilize higher power machineries. Multilevel inverters (MLI) are extensively applicable for higher power machineries due to the prolific benefits [1]-[3]. The inverters have the ability to provide required voltage and power by exploiting switching devices as an alternative for transformers. The THD and the electromagnetic interference in the output voltage and current waveform decreases as the number of output levels rises. The fundamental idea of the MLI is to obtain high power by utilizing power semiconductor switches with more than a few lower dc voltage sources. The deep-rooted topologies of MLI [4] have plentiful reward when compared to the traditional inverters. In recent days, the CHB inverter has become widely implemented topology for high-power variable-speed drive applications [5]-[7] such as conveyors, steel and paper rolling mills, locomotive traction drives, ship propulsion drives and battery operated and hybrid vehicle drives. The three phase CHB inverters are designed with a number of H-bridge units. The foremost emphasis is on the CHB-MLI for analyzing its performance with diverse current control methods including hysteresis current control [8]-[11], PI current control using SPWM technique [12], and predictive current control [13]-[17]. The main problem with hysteresis current control is its variable switching frequency that roots high switching losses and higher order harmonics in the load current, thereby increasing ripple current [18], [19]. The PI current controller has the problems of steady-state magnitude error, phase lag and limited disturbance rejection capability in controlling the load current [20], [21]. The current control methods are analyzed with the level of load current THD, reference current tracking capability and unbalanced load conditions. The five-level CHB inverter with the hysteresis, PI and predictive current control methods is simulated using the MATLAB Simulink.

The five-level CHB inverter topology is presented in section 2. The modulation techniques for CHB inverter are provided in section 3. The current control techniques are described in section 4. The simulation results are given in section 5 and the conclusion is drawn in section 6.

## 2. CHB INVERTER TOPOLOGY

The CHB inverter topology is formed by the sequence of H-bridge cells with individual DC voltage sources. A three-phase CHB inverter topology is formed by the series connection of H-bridge cells in each of the three phase legs as shown in Figure 1. The output voltage of the inverter is obtained by adding the voltages provided by the H-bridge cells. Three voltage levels,  $+V_{dc}$ , 0,  $-V_{dc}$  are provided by each individual single-phase H-bridge cell while linking the DC voltage to the output by diverse unions of power semiconductor switching devices ( $S_{A1}$ ,  $S_{A1'}$ ,  $S_{A2}$  and  $S_{A2'}$ ). A five-level CHB three-phase inverter with RL load is modeled for producing five level output voltage.

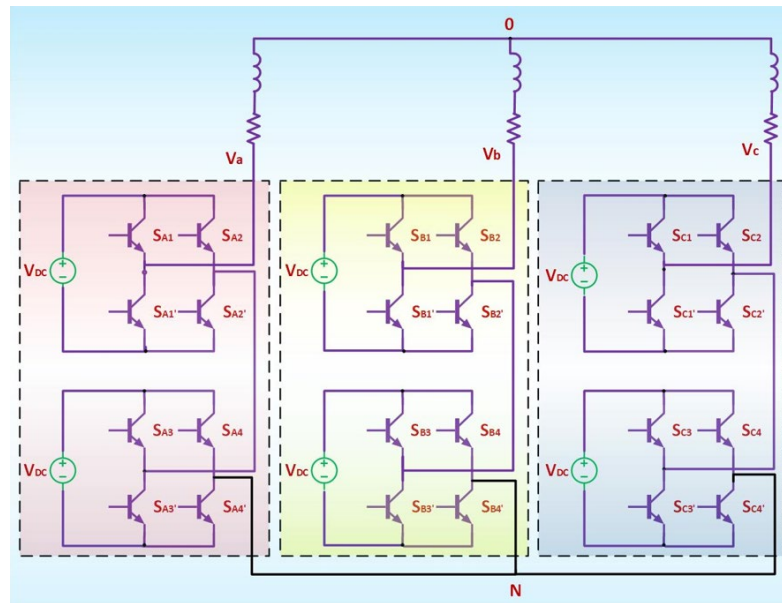


Figure 1. A five-level CHB three-phase inverter with RL load

## 3. MODULATION TECHNIQUES FOR CHB INVERTER

Numerous modulation methods [22]-[26] have been adopted for the CHB inverter based on specific requirements and distinctive applications. PS-PWM and LS-PWM are advancement of the conventional PWM techniques. Modulating signal of pure sinusoidal wave and multi carrier signals of triangular waves have been considered for generating the gate signals to the switching devices in the CHB inverter. The number of carrier signals needed for an m-level inverter is calculated by  $(m-1)$ . The  $(m-1)$  carrier signals are arranged in vertical shifts in LS-PWM technique. The PS-PWM method is implemented for generating gate signals to the inverter. The least THD for the inverter can be obtained when  $180$  or  $360/h$  (where  $h$  is the number of cells) phase shifts are provided between the carrier signals.

## 4. CURRENT CONTROL METHODS

### 4.1. Hysteresis controller

In the hysteresis current controller, the load current tracks the reference current within a hysteresis band. Figure 2(a) shows the block diagram of a hysteresis current controller for the inverter. The operating principle of the hysteresis modulation is shown in Figure 2(b). It has the upper and lower hysteresis band limits. When the load current surpasses the upper band limit, higher voltage level is selected until the current error reaches to zero. Similarly, When the load current surpasses the lower band limit, next voltage level is selected until the current error reaches to zero. Hence the load current is controlled within the upper and lower hysteresis band limits. The changes in the load parameters and operating constraints continuously modifies the switching frequency, which creates resonance problems and switching losses. This is considered as a main downside in the hysteresis current control method.

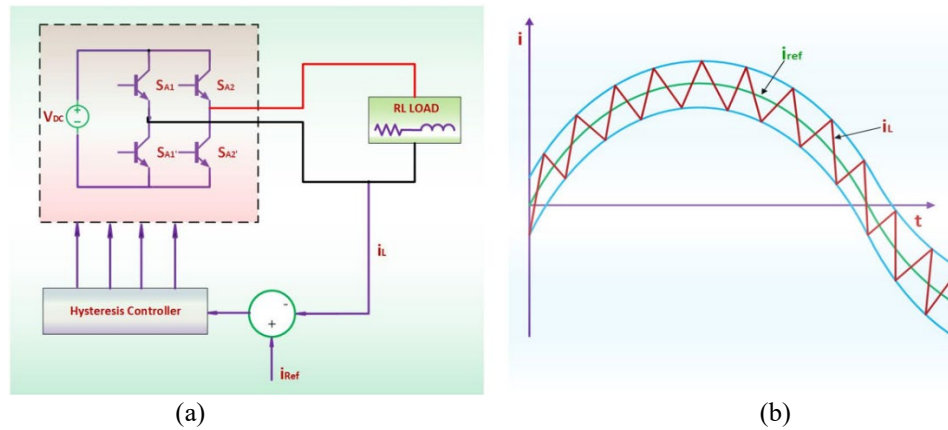


Figure 2. Hysteresis current controller (a) H-bridge cell with hysteresis controller and (b) Hysteresis current band

#### 4.2. Proportional-integral controller

The PI control method is a modest control technique with widespread industrial applications. The PI controller employing PSPWM is shown in Figure 3. The controller is comprised of a feedback loop for measuring the actual load current. The controller generates the reference voltages by processing the error between the reference current and the load current. The PSPWM scheme is used as a modulator to produce switching signals for the inverter.

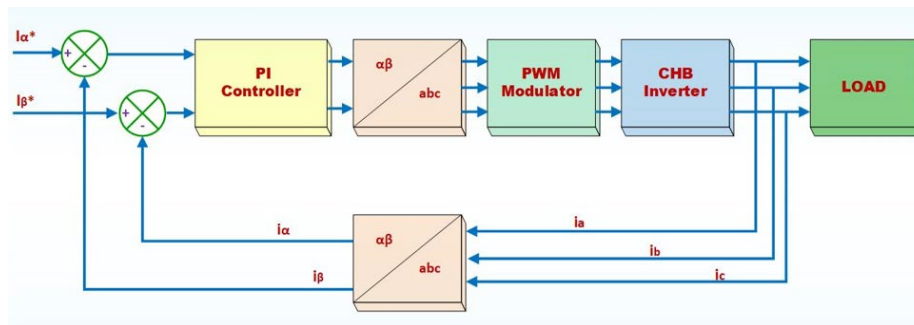


Figure 3. The block diagram of PI current controller

#### 4.3. Predictive control method

The predictive current control method [27] is a modern control technique that is expected to control the load current very effectively when compared with traditional control methods. The predictive current control method involves mathematical modeling of the CHB inverter and the predictive control model. The circuit diagram of the inverter with RL load as shown in the Figure 4 is used for mathematical modeling.

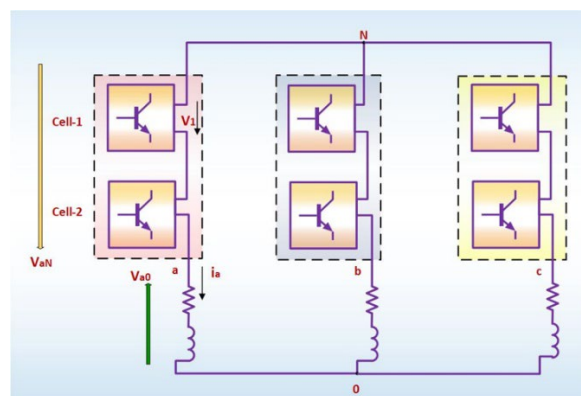


Figure 4. Circuit diagram of CHB three-phase inverter with RL load

#### 4.3.1. Modeling of CHB inverter

The probable voltage levels for each phase are:

$$m = 2h + 1 \quad (1)$$

where,  $m$  is count of voltage levels, and  $h$  is the count of H-Bridge cells per leg. The number of voltage level combinations  $L_m$  in the three-phase CHB inverter is:

$$L_m = m^3 \quad (2)$$

All the cells in the CHB inverter requires two gate pulses, the inverter voltage per leg is:

$$V_{aN} = V_{dc} \sum_{j=1}^h (S_{aj,1} - S_{aj,2}) \quad (3)$$

where,  $S_{aj,1}$  and  $S_{aj,2}$  are the gate pulses of the phase  $a$  and cell  $j$ . The conceivable switching amalgamation  $P_s$  is:

$$P_s = 2^{6h} \quad (4)$$

The differential equation for a leg of the  $RL$  load is:

$$V_{an}(t) = L \frac{di_a(t)}{dt} + Ri_a(t) \quad (5)$$

where,  $V_{an}$  is the potential difference with reference to neutral point of the load.

The potential difference across the load with respect to the inverter voltage is:

$$V_{a0} = V_{aN} + V_{n0} \quad V_{a0} = V_{aN} + V_{n0} \quad (6)$$

where,  $v_{n0}$  is the common-mode voltage ( $v_{cm}$ ), given by

$$V_{n0} = V_{cm} = \frac{V_{aN} + V_{bN} + V_{cN}}{3} \quad (7)$$

Using vectorial transformation, the load model is formulated as,

$$\begin{bmatrix} \alpha \\ \beta \end{bmatrix} = \begin{bmatrix} \frac{2}{3} & -\frac{1}{3} & -\frac{1}{3} \\ 0 & \frac{\sqrt{3}}{3} & \frac{\sqrt{3}}{3} \end{bmatrix} \begin{bmatrix} a \\ b \\ c \end{bmatrix} \quad (8)$$

where  $a$ ,  $b$ , and  $c$  are the three-phase parameters, and  $\alpha$  and  $\beta$  are the vectorial variables. In (5) can be formulated in relation to the vectorial variables  $\alpha$ - $\beta$  as,

$$V_{\alpha\beta}(t) = L \frac{di_{\alpha\beta}(t)}{dt} + Ri_{\alpha\beta}(t) \quad (9)$$

where  $i_{\alpha, \beta}$  is the current vector and  $V_{\alpha, \beta}$  is the voltage vector.

#### 4.3.2. Predictive current controller

In the predictive current controller shown in Figure 5, a mathematical model of the CHB inverter and the load is formulated to forecast the future behavior of the current for each and every diverse voltage vector produced by the inverter. The voltage vector that minimizes a cost function is nominated to be applied as a switching signal. The predictive current control method avoids the application of any modulation method in the CHB inverter.

Approximating  $di/dt$  in (9) by (10).

$$\frac{di_{\alpha\beta}}{dt} \approx \frac{i_{\alpha\beta}[k+1] - i_{\alpha\beta}[k]}{T_s} \quad (10)$$

and substituting it in (9), the forthcoming load current vector is obtained as (11).

$$i[k+1]_{\alpha, \beta} = \frac{T_s}{L} \left\{ V_{\alpha, \beta}[k] - i_{\alpha, \beta}[k] \left( R - \frac{L}{T_s} \right) \right\} \quad (11)$$

In (11) is implemented in the predictive controller to forecast the forthcoming value of the load current. The predicted load current values are evaluated using the given cost function so as to select the suitable voltage vectors for the current control.

$$g[k+1] = |i_{\alpha}^*[k+1] - i_{\alpha}[k+1]| + |i_{\beta}^*[k+1] - i_{\beta}[k+1]| \quad (12)$$

where  $i_{\alpha}^*[k+1]$  is the predicted reference current vector. For appropriately minor sampling times, it can be expected that  $i_{\alpha, \beta}^*[k+1] \approx i_{\alpha, \beta}^*[k]$ . The cost function in (12) is solved for all the conceivable voltage vector. The voltage vector which reduces the cost function is nominated and made functional.

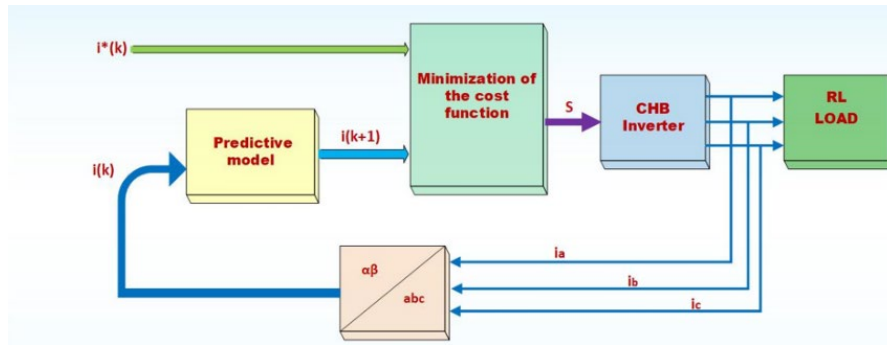


Figure 5. Block diagram of predictive current controller

## 5. SIMULATION RESULTS

The CHB inverter with different current control methods is simulated in MATLAB/Simulink software. The RL load is used to obtain simulation results. The parameters used for the simulation are specified in Table 1. The current control methods are examined and related with respect to current THD, varying reference current and unbalanced load conditions.

Table 1. Simulation parameters

Parameters	Values
Input voltage (Vdc)	45 V
Load resistance (R)	47 $\Omega$
Load inductance (L)	15 mH
Hysteresis Band Width ( $\delta$ )	$\pm 0.12$
Carrier frequency (PI controller)	2.5 KHz
Reference current	0.95

### 5.1. Current THD

The THD spectrum of the load current is evaluated with the aid of the FFT tool in MATLAB/Simulink. The THD level of the load current for various values of load are measured. The load current waveforms for hysteresis controller, PI controller, and predictive controller are shown in Figures 6, 7 and 8, respectively. The THD for different load values were compared as shown in the Figure 9 to analyze the effect of the hysteresis, PI, and predictive current control.

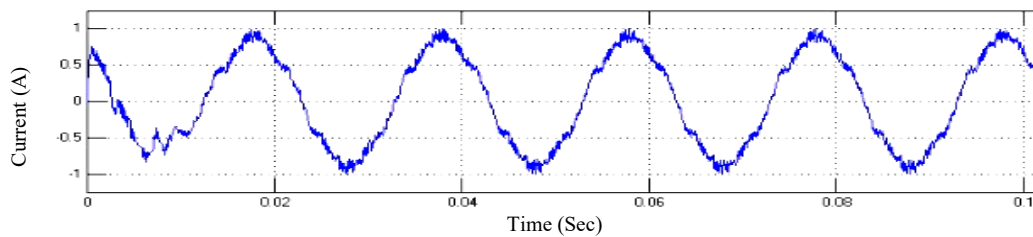


Figure 6. Load current waveforms for hysteresis controller

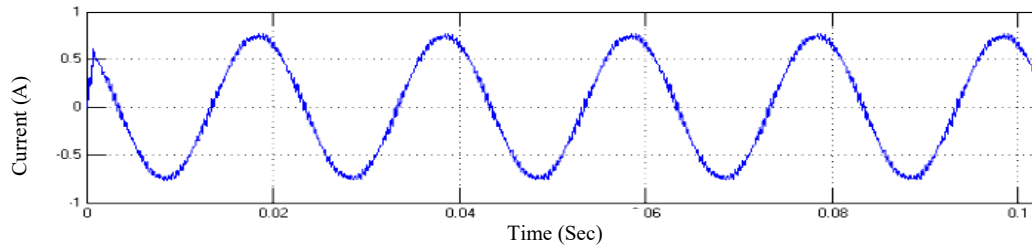


Figure 7. Load current waveforms for PI controller

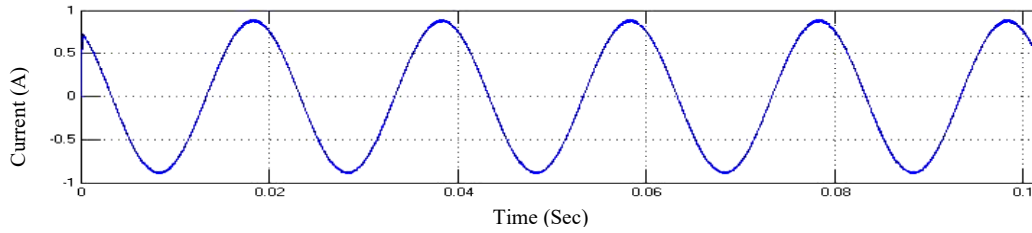


Figure 8. Load current waveforms for predictive controller

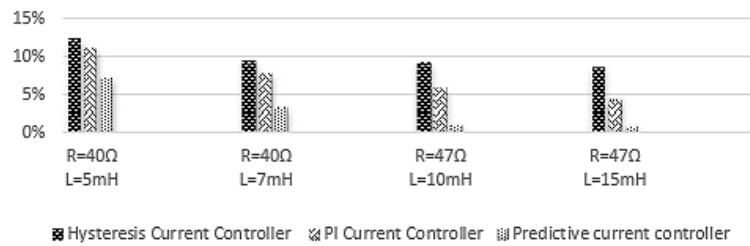


Figure 9. Comparison of current THD for hysteresis, PI, and predictive current controllers

## 5.2. Reference current variations

The amplitude of the reference current is varied from 0.9 A to 0.7 A at instant  $t = 0.04$  ms to 0.08 ms. The current tracking performance of the hysteresis control, PI control and predictive control methods are shown in Figures 10, 11, and 12, respectively. The Hysteresis current control method shows time lag in tracking the reference current, and has more current ripple. The PI control method shows phase lag in tracking the reference current. The predictive control method tracks the reference current perfectly when the reference current is varied.

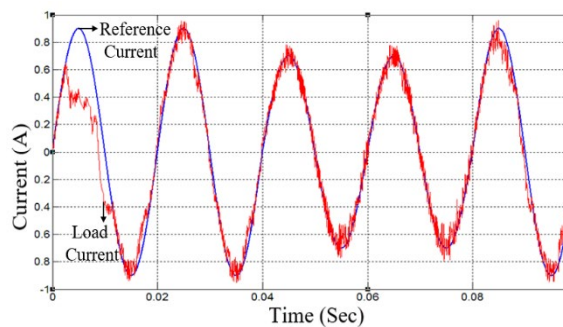


Figure 10. Current tracking for hysteresis controller

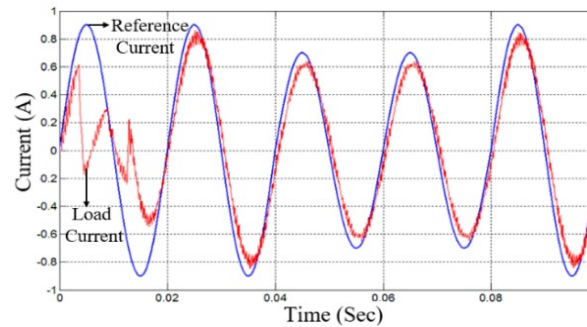


Figure 11. Current tracking for PI controller



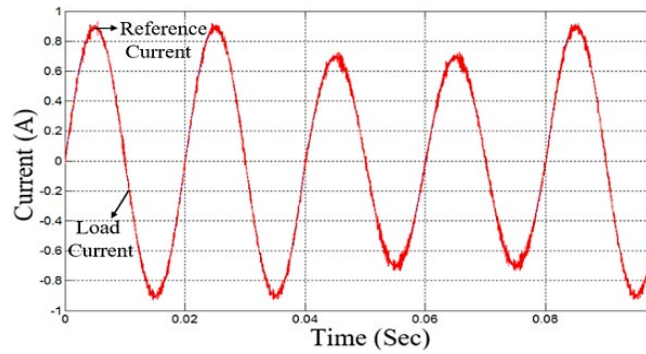


Figure 12. Current tracking for predictive controller

### 5.3. Unbalanced load condition

A three-phase load can be considered unbalanced when the phase impedances are not equal to each other. The magnitudes of each phase current are different. The response (load current) of the hysteresis control, PI control, and predictive control are shown in Figures 13, 14, and 15, respectively. The load values assumed for phase 'a' is  $R=42\ \Omega$ ,  $L=10\ \text{mH}$ , phase 'b' is  $R=47\ \Omega$ ,  $L=15\ \text{mH}$  and phase 'c'  $R=52\ \Omega$ ,  $L=20\ \text{mH}$ . The predictive current control method tracks the reference current perfectly during the unbalanced load currents.

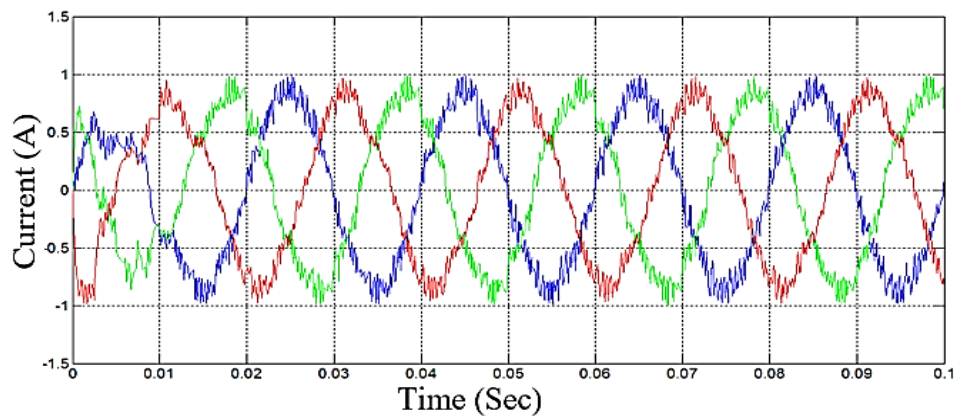


Figure 13. Response for hysteresis controller

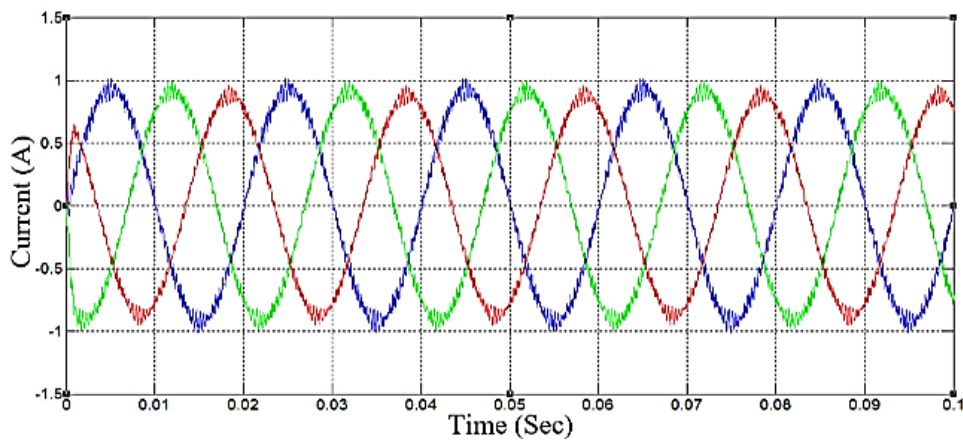


Figure 14. Response for PI controller

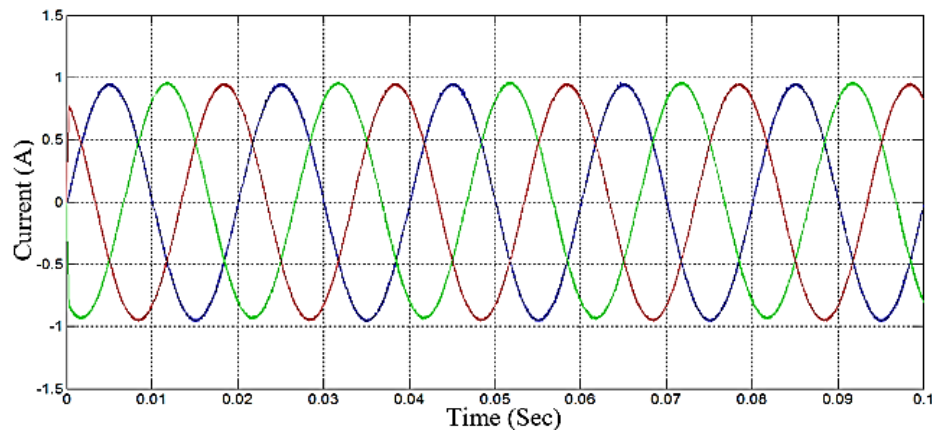


Figure 15. Response for predictive controller

## 6. CONCLUSION

The performance of hysteresis, PI and Predictive controller for the five-level CHB multilevel inverter were analyzed for various load conditions. The current THD spectra for the three control methods are compared, and the current spectrum attained with predictive current control method showed lower THD than the other two control methods. The simulation results for varying reference current shows more current ripple in the current tracked by hysteresis controller and phase lag in the current tracked by the PI controller. These two limitations are addressed by the predictive controller, and hence better performance of the predictive controller is observed in tracking the set reference current. When compared with other two current control methods, it is also noticed that the predictive controller effectively controls the load current within the preset limit during the unbalanced load conditions.

## REFERENCES




- [1] S. Kouro *et al.*, "Recent Advances and Industrial Applications of Multilevel Converters," *IEEE Trans. Ind. Electron.*, vol. 57, no. 8, pp. 2553–2580, Aug. 2010, doi: 10.1109/TIE.2010.2049719.
- [2] A. Krishna R. and L. P. Suresh *et al.*, "A brief review on multi level inverter topologies," *In Proceedings of the 2016 International Conference on Circuit, Power and Computing Technologies (ICCPCT)*, March 2016, pp. 1–6, doi: 10.1109/ICCPCT.2016.7530373.
- [3] S. Padmanaban and M. Pecht, "An isolated/non-isolated novel multilevel inverter configuration for a dual three-phase symmetrical/asymmetrical star-winding converter," *Engineering Science and Technology: An International Journal (JESTECH)*, vol. 19, no. 4, pp. 1763–1770, Aug. 2016, doi: 10.1016/j.jestech.2016.08.006.
- [4] I. Colak, E. Kabalci, and R. Bayindir, "Review of multilevel voltage source inverter topologies and control schemes," *Energy Convers. Manag.*, vol. 52, no. 2, pp. 1114–1128, 2011, doi: 10.1016/j.enconman.2010.09.006.
- [5] E. Babaei, S. Alilu, and S. Laali, "A New General Topology for Cascaded Multilevel Inverters with Reduced Number of Components Based on Developed H-Bridge," *IEEE Trans. Ind. Electron.*, vol. 61, no. 8, pp. 3932–3939, 2014, doi: 10.1109/TIE.2013.2286561.
- [6] K. Sivakumar, A. Das, R. Ramchand, C. Patel, and K. Gopakumar, "A Hybrid Multilevel Inverter Topology for an Open-End Winding Induction-Motor Drive Using Two-Level Inverters in Series with a Capacitor-Fed H-Bridge Cell," *IEEE Trans. on Industrial Electronics*, vol. 57, no. 11, pp. 3707–3714, Nov. 2010, doi: 10.1109/TIE.2010.2040565.
- [7] Y. Babkrani, A. Naddami, and M. Hilal, "A smart cascaded h-bridge multilevel inverter with an optimized modulation techniques increasing the quality and reducing harmonics," *International Journal of Power Electronics and Drive System (IJPEDS)*, vol. 10, no. 4, pp. 1852–1862, 2019, doi: 10.11591/ijpeds.v10.i4.pp1852-1862.
- [8] F. Wu, L. Zhang, and Q. Wu, "Simple unipolar maximum switching frequency limited hysteresis current control for grid-connected inverter," *IET Power Electron.*, vol. 7, no. 4, pp. 933–945, 2014, doi: 10.1049/iet-pel.2013.0284.
- [9] J. A. Suul, K. Ljokelsoy, T. Midtsund, and T. Undeland, "Synchronous Reference Frame Hysteresis Current Control for Grid Converter Applications," *IEEE Trans. Ind. Appl.*, vol. 47, no. 5, pp. 2183–2194, 2011, doi: 10.1109/TIA.2011.2161738.
- [10] R. Davoodnezhad, D. G. Holmes, and B. P. McGrath, "A Novel Three-Level Hysteresis Current Regulation Strategy for Three-Phase Three-Level Inverters," *IEEE Trans. Power Electron.*, vol. 29, no. 11, pp. 6100–6109, 2014, doi: 10.1109/TPEL.2013.2295597.
- [11] J. Zhang, H. Yang, T. Wang, L. Li, D. Dorrell, and D. D-C. Lu, "Field-oriented control based on hysteresis band current controller for a permanent magnet synchronous motor driven by a direct matrix converter," *IET Power Electron.*, vol. 11, no. 7, pp. 1277–1285, 2018, doi: 10.1049/iet-pel.2017.0651.
- [12] R. Tiwari, R. Babu N., R. Arunkrishna, and P. Sanjeevikumar, "Comparison between PI controller and Fuzzy logic-based control strategies for harmonic reduction in Grid integrated Wind energy conversion system," *Lecture Notes in Electrical Engineering Advances in Smart Grid and Renewable Energy*, Springer Journal Publications, Singapore, Dec. 2016, pp. 297–306, doi: 10.1007/978-981-10-4286-7\_29.
- [13] V. Yaramasu, M. Rivera, B. Wu, and J. Rodriguez, "Model Predictive Current Control of Two Level Four-Leg Inverters— Part I: Concept, Algorithm, and Simulation Analysis," *IEEE Trans. Power Electronics*, vol. 28, no. 7, July 2013, doi: 10.1109/TPEL.2012.2227509.
- [14] Y. Zhang, J. Zhu, and J. Hu, "Model predictive direct torque control for grid synchronization of doubly fed induction generator," in *Proc. 2011 IEEE Int. Electric Machines Drives Conf. (IEMDC)*, May 2011, pp. 765–770, doi: 10.1109/IEMDC.2011.5994908,






- [15] J. Rodriguez *et al.*, "State of the Art of Finite Control Set Model Predictive Control in Power Electronics," *IEEE Trans. Ind. Informatic*, vol. 9, no. 2, pp. 1003–1016, May 2013, doi: 10.1109/TII.2012.2221469.
- [16] P. Cortés, A. Wilson, S. Kouro, J. Rodriguez, and H. Abu-Rub, "Model Predictive Control of Multilevel Cascaded H-Bridge Inverters," *IEEE Trans. on Industrial Electronics*, vol. 57, no. 8, pp. 2691–2699, August 2010, doi: 10.1109/TIE.2010.2041733.
- [17] A. Iqbal, S. Moïnooddine, and K. Rahman, "Finite State Predictive Current and Common Mode Voltage Control of a Seven-phase Voltage Source Inverter," *International Journal of Power Electronics and Drive System (IJPEDS)*, vol. 6, no. 3, pp. 456–476, 2015, doi: 10.11591/ijpeds.v6.i3.pp459-476.
- [18] C. N. A. Julius, L. N. Muhammad, H. Daniyal, N. Jaalam, N. R. H. Abdullah, and S. Ab. Ghani, "A Comparative Study of Hysteresis Current Controller and PI Controller in Grid-Connected Inverter," *International Journal of Advanced Trends in Computer Science and Engineering*, vol. 8, no. 6, pp. 3182–3187, Dec., 2019, doi: 10.30534/ijatcse/2019/83862019.
- [19] T. Nguyen-Van, R. Abe, and K. Tanaka, "A Digital Hysteresis Current Control for Half-Bridge Inverters with Constrained Switching Frequency," *Energies*, vol. 10, no. 10, pp. 1–13, 2017, doi: 10.3390/en10101610.
- [20] M. Parveza, M. F. M. Elias, and N. A. Rahim, "Performance analysis of PR current controller for single-phase inverters," *4th IET Clean Energy and Technology Conference (CEAT 2016)*, 2016, doi: 10.1049/cp.2016.1311.
- [21] T. C. A. Ajot, S. Salimin, and R. Aziz, "Application of PI Current Controller in Single Phase Inverter System Connected to Non-Linear Load," *IOP Conference Series: Materials Science and Engineering*, vol. 226, no. 1, August 2017, pp. 1-8, doi: 10.1088/1757-899X/226/1/012135.
- [22] A. Boulahia, M. Adel, and H. Benalla, "Predictive Power Control of Grid and Rotor Side converters in Doubly Fed Induction Generators Based Wind Turbine," *Bulletin of Electrical Engineering and Informatics*, vol. 2, no. 4, pp. 258–264, 2013, doi: 10.11591/eei.v2i4.191.
- [23] M. Kanimozhi and P. Geetha, "A new boost switched capacitor multilevel inverter using different multi carrier PWM techniques," in *Proceedings of the 2014 International Conference on Circuits, Power and Computing Technologies [ICCPCT-2014]*, Nagercoil, India, 20–21 March 2014, pp. 432–437, doi: 10.1109/ICCPCT.2014.7054905.
- [24] P. Sanjeevikumar, F. Blaabjerg, P. Wheeler, V. Fedák, M. J. Duran, and P. Siano, "A Novel Five-level Optimized Carrier Multilevel PWM Quad-Inverter Six-Phase Asymmetrical AC Drive," in *2016 IEEE International Power Electronics and Motion Control Conference (PEMC)*, Varna (Bulgaria), 25–30 Sept. 2016, pp. 26–31, doi: 10.1109/EPEPEMC.2016.7751969.
- [25] M. Nagaraju and M. K. Kumar, "Analysis of series/parallel multilevel inverter with symmetrical and asymmetrical configurations," *International Journal of Power Electronics and Drive System (IJPEDS)*, vol. 10, no. 1, pp. 300–306, March 2019, doi: 10.11591/ijpeds.v10.i1.pp300-306.
- [26] Sundararajan K, A. Nachiappan, and Veerapathiran G., "Comparison of Current Controllers for a Five-level Cascaded H-Bridge Multilevel Inverter," *International Journal of Computational Engineering Research (ijceronline.com)*, vol. 2, no. 6, pp. 55–62, October 2012, doi: 10.1.1.412.2718.
- [27] J. Rodriguez and P. Cortes, "Predictive Control of Power Converters and Electrical Drives," *Wiley-IEEE Press*, April 2012.

## BIOGRAPHIES OF AUTHORS



**Prem Sunder Gnanamurthy**    received the B.E. degree in Electrical and Electronics Engineering from Madras University in 2002, and the M.Tech. in Electrical Drives and control from Pondicherry University in 2006 and completed his Ph.D. at Annamalai University in 2017. He is having 14 years of experience and presently working as Professor in the Department of Electrical and Electronics Engineering at Mailam Engineering College, Mailam. His research interests include Multilevel Inverter, DC-DC Converter and Z-Source and Quasi-Z-source converters. He can be contacted at email: premgsunder@gmail.com.



**Veerapathiran Govindasamy**    received the B.E. degree in electrical and electronics engineering from Anna University, Chennai in 2010 and the M.Tech degree from Pondicherry University in 2013. He has held a position as an Assistant Professor at Mailam Engineering College for five years. He is currently a Senior Consultant (Innovation and Technology) with Learning Links Foundation, New Delhi, India. His main research interests are the Electrical Drives, Renewable Energy, Multilevel Inverters, DC-DC Converters and Model Predictive Control. He can be contacted at email: veerapec2012@gmail.com.